Synthesis and Characterization of Gold/Polypyrrole Core−Shell Nanocomposites and Elemental Gold Nanoparticles Based on the Gold-Containing Nanocomplexes Prepared by Electrochemical Methods in Aqueous Solutions

Yu-Chuan Liu*,† and Thomas C. Chuang‡

Department of Chemical Engineering and Polymer Material R&D Center, Van Nung Institute of Technology, 1, Van Nung Road, Shuei-Wei Li, Chung-Li City, Taiwan, Republic of China

Received: June 12, 2003; In Final Form: September 22, 2003

We report here the first electrochemical pathway to prepare Au-containing nanocomplexes with the mean diameter of 2 nm in 0.1 N KCl aqueous solutions without addition of any stabilizer. Encouragingly, polypyrrole-(PPy-) coated gold nanocomposites with a core−shell structure and a diameter smaller than 8 nm can be prepared by the formation of self-assembled monolayers and further orderly autopolymerization of pyrrole monomers on these nanocomplexes. The prepared Au/PPy nanocomposites should exhibit extremely high conductivity, as indicated by the analyses of X-ray diffraction (XRD), X-ray photoelectron spectroscopy (XPS), and surface-enhanced Raman scattering (SERS). Meanwhile, elemental Au(0) nanoparticles of a mean diameter of 5 nm can be obtained by treating the Au/PPy-nanocomposites-containing solution with sonification.

Introduction

The fabrication of materials with nanometer-sized dimensions has become an important branch of research.[1,2] Recently, nanoparticles of noble metals are attracting much attention from scientific and technological viewpoints because of their interesting optical,[3] electrochemical,[4] photoelectrochemical,[5] and electronic[6] properties. Methods to nanoparticles fabrication include chemical reduction,[7] sonochemical reduction,[8] laser ablation,[9] radiolytic reduction,[10] metal evaporation,[11] and Ar^+ ion sputtering,[6] etc. However, the metal nanoparticles are only stable as suspensions in solutions and tend to irreversibly aggregate over time. This nature depresses their nanoscale properties and limits their applications. Therefore, some stabilizers, sodium dodecyl sulfate[8] and sugar ball,[12] were used, and some stabilization technologies of thiol-ligand coatings[13,14] were developed to prevent the prepared nanoparticles from aggregation. The latter is derived from the application of self-assembled monolayers (SAMs). SAMs are formed by the spontaneous adsorption of organic molecules onto a metal or metal oxide surface, especially for alkanethios adsorbing on copper, silver and particular gold.[15,16] On these metals, thiols form a densely packed, oriented monolayer. The assemblies are the product of strong metal−sulfur interactions that are also responsible for the robust nature of the SAM in liquid. Also, the application of diblock copolymers was reported to provide small compartments, inside which nanoparticles can be formed and stabilized.[17] In the previous studies of SERS spectroscopy of PPy,[18,19] we reported the evidence of chemical effect on SERS of PPy electrodeposited on gold roughened by electrochemical oxidation−reduction cycles (ORC) and the relationship between crystalline orientations of gold and SERS of PPy deposited on it. Encouragingly, during roughening Au substrates by the ORC treatment, stable Au-containing nanocomplexes are found existing in a 0.1 N KCl aqueous solution without any other additive. Most of the researches on SERS are generally focused on the surface of roughened substrates.[20,21] These novel nanocomplexes existing in aqueous solutions with very palely yellow color are usually ignored. Meanwhile, these nanocomplexes, which are distinguishable from the elemental metal nanoparticles generally reported in the literature, can not only adsorb adsorbates to form SAMs but also oxidize them due to their electrochemical activities, as discussed later.

Experimental Section

The electrochemical system used for the experiments was shown elsewhere.[18,19] During the ORC treatment, the Au substrate was cycled in a deoxygenated aqueous solution containing 0.1 N KCl from −0.28 to +1.22 V vs Ag/AgCl at 500 mV/s with 25 scans. The durations at the cathodic and anodic vertexes are 10 and 5 s, respectively. Then the $AuCl_4^-$ nanocomplexes were prepared in this aqueous solution. Subsequently, 0.2 mmol/L pyrrole monomers was added into this $AuCl_4^-$-containing aqueous solution, and the mixture was stirred for 1 h at room temperature to prepare Au/PPy nanocomposites. Then this Au/PPy-nanocomposites-containing solution was placed in an ultrasonic bath for 30 min to prepare elemental Au(0) nanoparticles.

The XRD pattern of the Au/PPy nanocomposites was recorded with a Philips X'Pert instrument using Cu Kα. A single drop of the sample-containing solution was placed on a 300 mesh Cu/carbon film TEM sample grid and allowed to be dried in a vacuum oven. Then the sample was examined using a JEOL JEM-4000 EX electron microscope with an acceleration voltage of 400 kV. Before recording the XPS spectra, a few drops of samples were evaporated on an amorphized graphite substrate. A Physical Electronics PHI 1600 spectrometer with monochromatized Mg Kα radiation at 15 kV 250 W and an energy resolution of 0.1−0.8% $\Delta E/E$ was used. Ultraviolet−visible absorption spectroscopic measurements were carried out on a Perkin-Elmer Lambda 25 spectrophotometer in 1 cm quartz curvettes.

* Corresponding author. Telephone: 886-3-4515811 ext540. Fax: 886-2-86638557. E-mail: liuyc@cc.vit.edu.tw.

† Department of Chemical Engineering, Van Nung Institute of Technology.

‡ Polymer Material R&D Center, Van Nung Institute of Technology.

10.1021/jp035680h CCC: $25.00
Published on Web 10/16/2003

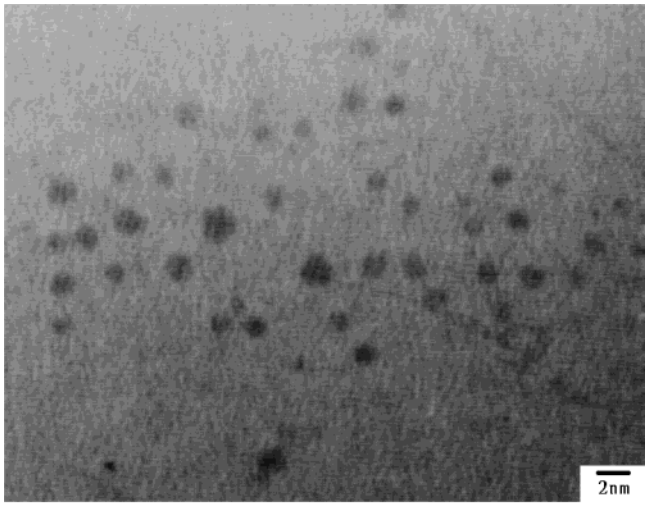

(a)

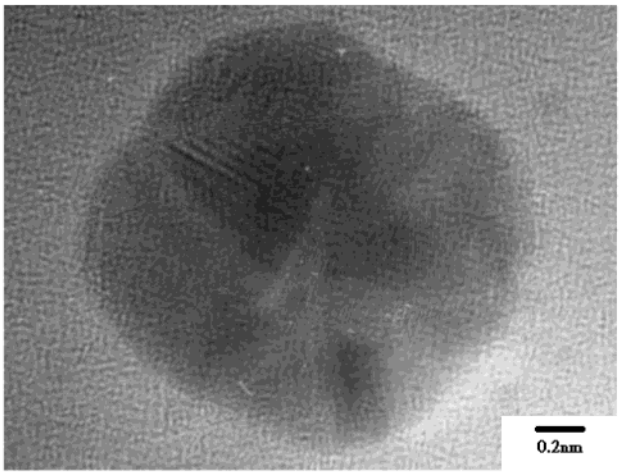

(b)

Figure 1. TEM micrograph of Au-containing nanocomplexes, showing (a) size and dispersion and (b) moiré fringes.

Results and Discussion

The dispersion and the particle size of Au-containing nanocomplexes existing in a 0.1 N KCl aqueous solution, after roughening the Au substrate by the ORC treatment for 25 times, are examined by using the transmission electron microscopy (TEM), as shown in Figure 1a. The nanocomplexes with a mean diameter of ca. 2 nm demonstrate no aggregation and fairly even dispersion. However, they exhibit nonperfectly spherical shapes because they are composed of positively charged Au and negatively charged Cl, which can be confirmed from the XPS analysis and from the UV−vis adsorption spectrum. Because the XPS spectra are similar to those observed on the roughened Au substrates, as shown before,[18,19] they can be assigned to $AuCl_4^-$. However, since the spectra would be featureless in a TEM image if the solution only contains $AuCl_4^-$ ions and the UV−vis absorption spectrum, as shown later, reveals that the particles on the surface of the Au-containing nanocomplexes would not be zerovalent Au, the structure of the Au-containing nanocomplexes prepared in this study may be proposed as small clusters of zerovalent Au with a shell of $AuCl_4^-$. Figure 1b shows the moiré patterns of the $AuCl_4^-$ nanocomplexes. It exhibits an one-dimensional fringe lattice due to moiré interference, indicating that these nanocomplexes are in themselves crystalline.[13]

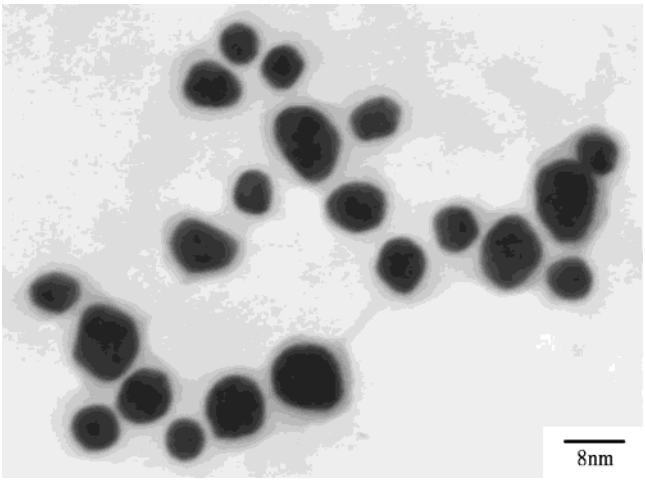

Figure 2. TEM micrograph of Au/PPy core−shell nanocomposites.

Figure 2 shows the micrograph of the forming Au/PPy core−shell nanocomposites after 0.2 mmol/L pyrrole monomer was added into the $AuCl_4^-$-containing aqueous solution and the mixture was stirred for 1 h at room temperature. Actually, the autopolymerization of pyrrole into PPy and the reduction of $AuCl_4^-$ to elemental Au occur instantaneously and simultaneously after the addition of pyrrole monomers, as inferred from the appearance of the characteristically clear black solution. The size distributions are relatively wide and the shapes are somewhat elongated due to the oxidation polymerization of pyrrole occurring on multiple $AuCl_4^-$ nanocomplexes, instead of an individual $AuCl_4^-$ nanocomplex. Distinguishable dark cores surrounded by grayish shells of PPy show that Au/PPy core−shell nanocomposites with diameters less than 8 nm can be successfully prepared. The Au in these nanocomposites is zerovalent, as revealed from the XPS analysis. To further obtain elemental Au(0) nanoparticles, the Au/PPy nanocomposites-containing solution was treated with sonification at room temperature for 30 min. The ultrasonic generator was operated at 40 kHz with an input power of 130 W. Then the desorbed PPy powders were removed from Au nanoparticles by using several centrifugation cycles. The obtained elemental Au(0) nanoparticles without a shell of PPy were examined by the TEM analysis. The TEM images show that the mean diameter of these nanoparticles is 5 nm. The XPS analysis further confirms that these nanoparticles are free of PPy.

Figure 3 shows the XPS Au $4f_{7/2-5/2}$ core-level spectra of the $AuCl_4^-$ nanocomplexes, the Au/PPy nanocomposites and the elemental Au(0) nanoparticles. As shown in spectra b and c, the doublet peaks located at 84 and 87.7 eV can be assigned to Au(0).[22] As comparing spectrum a, representing the $AuCl_4^-$ nanocomplexes, with spectrum b or c, representing the elemental nanoparticles Au(0), it is found that there are extra oxidized components of Au shown in the higher binding energy side. The oxidized Au shown in spectrum a can be assigned to monovalent Au(I) and trivalent Au(III) at 85.2 and 86.7 eV, respectively.[23] No further deconvolution was made, and trivalent Au(III), as usually shown in the Cl- and Au-containing complex,[22,24] was adopted in this study. As shown in spectrum a of Figure 4, the absorbance maximum of $AuCl_4^-$ nanocomplexes appears approximately at 308 nm, which is markedly different from that of zerovalent Au located at ca. 520 nm.[25,26] After addition of pyrrole monomers, the absorbance at 308 nm disappears, and a new band of $\pi-\pi^*$ transition of PPy[27] in the region of 400−500 nm with absorbance maximum at ca. 463 nm arises instead, as shown in spectrum b of Figure 4. It

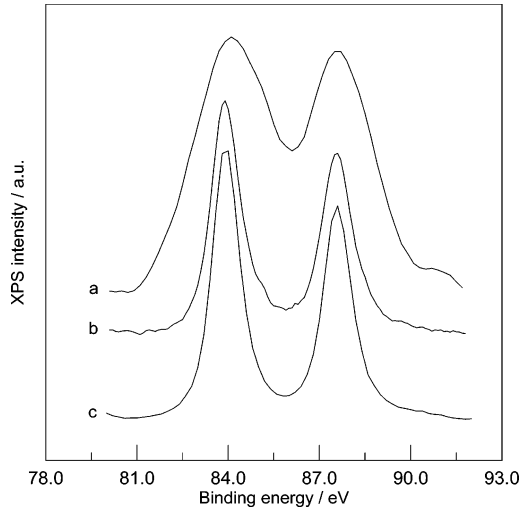

Figure 3. XPS Au $4f_{7/2-5/2}$ core-level spectra of $AuCl_4^-$ nanocomplexes (curve a), Au/PPy core−shell nanocomposites (curve b), and elemental Au(0) nanoparticles (curve c) after treating the Au/PPy core−shell nanocomposites with sonification for 30 min.

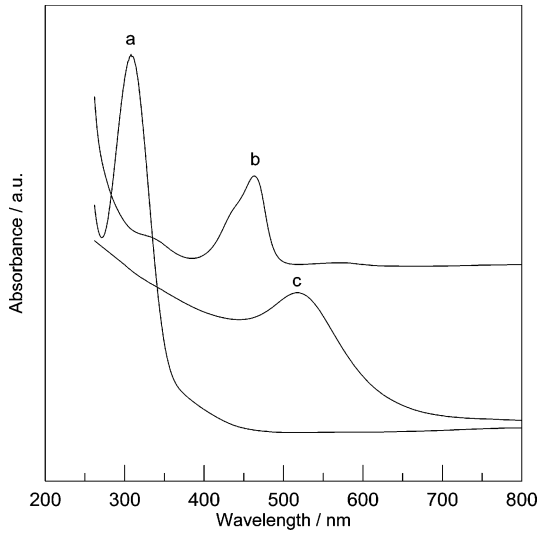

Figure 4. UV−vis spectra of Au-containing colloidal solutions: (a) Au-containing nanocomplexes; (b) Au/PPy core−shell nanocomposites; (c) elemental Au(0) nanoparticles after treating Au/PPy core−shell nanocomposites with sonification for 30 min.

indicates that the Au/PPy nanocomposites with a core−shell structure have been successfully prepared. Correspondingly, the appearance of the characteristic absorbance maximum at ca. 517 nm, as shown in spectrum c of Figure 4, reveals that the elemental Au(0) nanoparticles free of PPy are readily prepared.

Further XRD examination of the $AuCl_4^-$ which is formed after the ORC treatment, as compared to that of the bulk Au substrate before the ORC treatment, reveals some interesting phenomena. The result indicates that the (220) face of the bulk Au substrate was partially changed into the (111) face, which corresponds to the lowest surface energy,[28] of the forming $AuCl_4^-$ after the ORC treatment. Highly ordered monolayer films were found to be self-assembled onto Au(111) in the study by Caldwell et al.[29] Before the formation of the Au/PPy nanocomposites, the pyrrolylium nitrogen inclines to adsorb along the (111) face with the lowest surface energy on the $AuCl_4^-$ to form ordered SAMs.[30,31] Due to different chemical natures between them, the electron charge transfer occurs from the pyrrolylium nitrogen to the $AuCl_4^-$ nanocomplexes. The resulting Au/PPy nanocomposites demonstrate a marked order

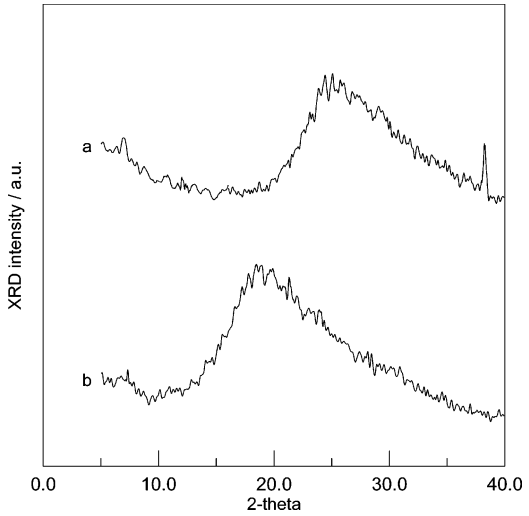

Figure 5. XRD patterns of PPy: (a) Au/PPy core−shell nanocomposites; (b) pure PPy film electrodeposited on Au substrate.

in character, as displayed in pattern a of Figure 5. The broad maximum of 2θ at ca. 25.1° (3.5 Å) is associated with the closest distance of approach of the planar aromatic rings of pyrrole, like face-to-face pyrrole rings.[32] However, the lower angle maximum of 2θ at ca. 19.0° (4.7 Å) for the generally electrodeposited PPy, as shown in pattern b of Figure 5, means scattering from side-by-side pyrrole rings.[32] Meanwhile, the corresponding coherence lengths, which are calculated from the Sherrer equation,[33] of the Au/PPy nanocomposites and the electrodeposited PPy, as prepared for comparison, are 11.03 and 9.73 Å, respectively. The higher coherence length indicates the increased crystallinity and crystalline coherence, which would contribute to the higher conductivity of PPy.[34,35] Due to the quantity limitation of the formation of Au/PPy nanocomposites, the real conductivity cannot be directly obtained by the four-probe technique measuring on the pellets of the samples. However, the XPS result of high oxidation level[19] of 0.33 and the SERS result of C=C backbone stretching[36] located at 1590 cm^{-1} of the prepared Au/PPy nanocomposites also show that they have extremely high conductivities.

We have found the electrochemical activities of $AuCl_4^-$ nanocomplexes existing in the aqueous solution during ORC treatment for roughening Au substrate. They can be used to fabricate Au/PPy core−shell nanocomposites with extremely high conductivities and further prepare elemental Au(0) nanoparticles. The study on the potential application of this methodology to other S- or N-containing conducting or functional group polymers is currently underway.

Acknowledgment. The authors thank the National Science Council of the Republic of China (NSC-91-2214-E−238-001) and Van Nung Institute of Technology for their financial support.

References and Notes

(1) Shon, Y. S.; Wuelfing, W. P.; Murray, R. W. *Langmuir* **2001**, *17*, 1255.

(2) Rodriguez, J. A.; Liu, G.; Jirsak, T.; Hrbek, J.; Chang, Z.; Dvorak, J.; Maiti, A. *J. Am. Chem. Soc.* **2002**, *124*, 5242.

(3) Templeton, A. C.; Pietron, J. J.; Murray, R. W.; Mulvaney, P. *J. Phys. Chem. B* **2000**, *104*, 564.

(4) Demaille, C.; Brust, M.; Tsionsky, M.; Bard, A. J. *Anal. Chem.* **1997**, *69*, 2323.

(5) Chandrasekharan, N.; Kamat, P. V. *J. Phys. Chem. B* **2000**, *104*, 10851.

(6) Peto, G.; Molnar, G. L.; Paszti, Z.; Geszti, O.; Beck, A.; Guczi, L. *Mater. Sci. Eng., C* **2002**, *19*, 95.
(7) Zheng, J.; Zhu, Z.; Chen, H.; Liu, Z. *Langmuir* **2000**, *16*, 4409.
(8) Mizukoshi, Y.; Okitsu, K.; Maeda, Y.; Yamamoto, T. A.; Oshima, R.; Nagata, Y. *J. Phys. Chem. B* **1997**, *101*, 7033.
(9) Dolgaev, S. I.; Simakin, A. V.; Voronov, V. V.; Shafeev, G. A.; Verduraz, F. B. *Appl. Surf. Sci.* **2002**, *186*, 546.
(10) Henglein, A.; Meisel, D. *Langmuir* **1998**, *14*, 7392.
(11) Bourg, M. C.; Badia, A.; Lennox, R. B. *J. Phys. Chem. B* **2000**, *104*, 6562.
(12) Esumi, K.; Hosoya, T.; Suzuki, A.; Torigoe, K. *Langmuir* **2000**, *16*, 2978.
(13) Sarathy, K. V.; Raina, G.; Yadav, R. T.; Kulkarni, G. U.; Rao, C. N. R. *J. Phys. Chem. B* **1997**, *101*, 9876.
(14) Zamborini, F. P.; Gross, S. M.; Murray, R. W. *Langmuir* **2001**, *17*, 481.
(15) Schoenfisch, M. H.; Pemberton, J. E. *J. Am. Chem. Soc.* **1998**, *120*, 4502.
(16) Huang, K.; Wan, M. *Chem. Mater.* **2002**, *14*, 3486.
(17) Antonietti, M.; Forster, S.; Hartmann, J.; Oestreich, S. *Macromolecules* **1996**, *29*, 3800.
(18) Liu, Y. C.; Jang, L. Y.*J. Phys. Chem. B* **2002**, *106*, 6748.
(19) Liu, Y. C. *Langmuir* **2002**, *18*, 174.
(20) Lu, P.; Dong, J.; Toshima, N. *Langmuir* **1999**, *15*, 7980.
(21) Hesse, E.; Creighton, J. A. *Langmuir* **1999**, *15*, 3545.
(22) Henry, M. C.; Hsueh, C. C.; Timko, B. P.; Freund, M. S. *J. Electrochem. Soc.* **2001**, *148*, D155.
(23) Suzer, S.; Ertas, N.; Kumser, S.; Ataman, O. Y. *Appl. Spectrosc.* **1997**, *51*, 1537.
(24) Gao, P.; Gosztola, D.; Leung, L. W. H.; Weaver, M. J. *J. Electroanal. Chem.* **1987**, *233*, 211.
(25) Dawson, A.; Kamat, P. V. *J. Phys. Chem. B* **2001**, *105*, 960.
(26) Ship, A. N.; Lahav, M.; Gabai, R.; Willner, I. *Langmuir* **2000**, *16*, 8789.
(27) Street, G. B.; Clarke, T. C.; Krounbi, M.; Kanazawa, K.; Lee, V.; Pfluger, P.; Scott, J. C.; Weiser, G. *Mol. Cryst. Liq. Cryst.* **1982**, *83*, 253.
(28) Chen, J. S.; Devine, T. M.; Ogletree, D. F.; Salmeron, M. *Surf. Sci.* **1991**, *258*, 346.
(29) Caldwell, W. B.; Campbell, D. J.; Chen, K.; Herr, B. R.; Mirkin, C. A.; Malik, A.; Durbin, M. K.; Dutta, P.; Huang, K. G. *J. Am. Chem. Soc.* **1995**, *117*, 6071.
(30) Frankamp, B. L.; Bial, A. K.; Rotello, V. M.*J. Am. Chem. Soc.* **2002**, *124*, 15146.
(31) He, H. X.; Zhang, H.; Li, Q. G.; Zhu, T.; Li, S. F. Y.; Liu, Z. Z. *Langmuir* **2000**, *16*, 3846.
(32) Mitchell, G. R. *Polym. Commun.* **1986**, *27*, 346.
(33) Alexander, L. E. *X-ray Diffraction Methods in Polymer Science*; Wiley-Interscience: New York, 1976; Chapter 7.
(34) Mo, Z.; Lee, K. B.; Moon, Y. B.; Kobayashi, M.; Heeger, A. J.; Wudl, F. *Macromolecules* **1985**, *18*, 1972.
(35) Allen, N. S.; Murray, K. S.; Fleming, R. J.; Saunders, B. R. *Synth. Met.* **1997**, *87*, 237.
(36) Liu, Y. C.; Hwang, B. J. *Synth. Met.* **2000**, *113*, 203.